

Article

# Overall Stability Valorization of Printed Sustainable Packaging Paper Containing Triticale Straw Pulp

Maja Rudolf \*, Ivana Plazonić, Katja Petric Maretić and Irena Bates

Faculty of Graphic Arts, University of Zagreb, 10000 Zagreb, Croatia; ivana.plazonic@grf.unizg.hr (I.P.); katja.petric.maretic@grf.unizg.hr (K.P.M.); irena.bates@grf.unizg.hr (I.B.)

\* Correspondence: maja.rudolf@grf.unizg.hr

**Abstract:** Due to the rising problem of deforestation, slow renewability, and higher cost of wood sources, it is of great importance for the paper and packaging industry to find suitable, environmentally friendly alternative sources of cellulose fibers. Much of the research has focused on studying the use of non-wood sources from various annual or perennial plants from which cellulose fibers can be obtained with equal quality to those from wood sources, since they are a fast-growing, renewable, and cheap source of fibers. This research focuses on the laboratory production and stability valorization of a paper substrate for packaging containing virgin fibers from triticale straw mixed with recycled wood pulp in various amounts up to 30%, printed with black ink through a simulation of the offset printing technique under controlled conditions. For stability analysis, printed paper substrates were subjected to three treatments essential for packaging: aging, rubbing, and chemical treatment. The stability of the prints was evaluated after treatments through spectrophotometric measurements ( $\Delta E^*_{ab}$ ,  $\Delta R$ ,  $\Delta L^*$ ,  $\Delta a^*$ ,  $\Delta b^*$ ) and Fourier transform infrared analysis. The aging, rubbing, and chemical stability of the prints with the addition of triticale virgin fibers was improved for all product packaging except for products containing soybean oil.

**Keywords:** offset printing; packaging; paper substrate; stability; triticale straw pulp

**Citation:** Rudolf, M.; Plazonić, I.; Petric Maretić, K.; Bates, I. Overall Stability Valorization of Printed Sustainable Packaging Paper Containing Triticale Straw Pulp. *Processes* **2023**, *11*, 1465. <https://doi.org/10.3390/pr11051465>

Academic Editor: Pavel Mokrejš

Received: 7 April 2023

Revised: 1 May 2023

Accepted: 9 May 2023

Published: 11 May 2023



**Copyright:** © 2023 by the authors. Licensee MDPI, Basel, Switzerland. This article is an open access article distributed under the terms and conditions of the Creative Commons Attribution (CC BY) license (<https://creativecommons.org/licenses/by/4.0/>).

## 1. Introduction

The packaging industry is facing great changes due to the increasing demand for sustainable packaging with a low environmental impact. Consumers' awareness of environmentally friendly products and packaging is increasing [1]; thus, the packaging needs to reflect the products' intentions through selecting appropriate materials with an emphasis on the ecological aspect of production and its biodegradability through explicit design [2]. Paper is a material that has the potential to replace other types of packaging such as plastic due to its biodegradability and recyclability, as well as consumer perception of its sustainability [3]. The production of paper and board for packaging has been steadily increasing over the past decade, even though overall paper and board production is on the decline. The global pandemic has also brought drastic changes in consumers' shopping habits, which entailed increased production of paper and board packaging by 7.1% in 2021 compared to the previous year in CEPI member countries, but the reports for 2022 show a decline of 4.6%. The main reason for the decrease in production is caused by the shortage of raw materials and high utility prices [4], but the overall demand remained stable. Statistical reports show that in the European Union (27 countries), the average generation of paper and cardboard waste increased to 43,490,000 tons (97 kg per capita) in 2020 [5], of which packaging waste made up an average of 73.11 kg per capita, while 59.59 kg per capita ended up in the recycling process [6]. Due to the high demand for paper packaging and the relative scarcity of virgin raw materials, it is necessary that all available sources are utilized in paper production. It is known that recycled papers are relatively

widely used, mainly for ecological and economic reasons. They are produced from secondary, already used, old paper fibers. The recycling process itself involves repulping the recovered paper to reduce it to fiber pulp, separating the ink from the fiber, and removing the ink particles from the stock, which is then converted into paper using a conventional papermaking machine. This process damages and shortens the fibers, meaning they cannot be recycled endlessly [7]. Therefore, the potential of recycled pulp can be maximized by mixing it with a virgin pulp of appropriate properties [8]. Thus, it is important to continuously incorporate a certain amount of virgin fibers into the pulp of recycled fiber for strength, quality, and availability reasons. Therefore, it is clear that the paper industry cannot rely solely on waste paper as the only source of fiber, and this cannot be used effectively for all paper grades. The scarcity of native pulpwood resources in some parts of the world and the focus of wood raw materials on higher-value-added products such as furniture have led the paper and packaging industry to focus more on alternative sources of cellulose fibers [9].

As a logical alternative to wood raw materials for the production of fibers, pulp, and paper, by-products from field production were imposed due to their numerous advantages. In almost all countries with favorable agro-climatic conditions, cereals are grown for human consumption, with a large amount of straw produced in fields after harvest. If we take into account that the straw to grain ratio is, on average, 1.5:1 [10], a very large amount of straw as residues, accumulated after the harvest of annual plants, is available annually. The basic requirement for an alternative plant to be used as a raw material for the paper industry is a sufficient amount of cellulose, and the cellulose content in this non-wood raw material is generally about 50%, which is approximately the same as in wood [11]. However, due to the pronounced heterogeneity of cellulose due to the growth conditions with a short cultivation period (annual plants), the use of this type of raw material for the production of cellulose lags far behind wood raw material. On the other hand, the low lignin content, which ensures energy and chemical savings during the pulp production process, makes this raw material extremely potential from an ecological point of view [12]. Since not all types of paper can be produced from any fibrous raw material, it is very important to reconsider the possibilities of using straw in paper production, but also the printability of such substrates.

In this study, we analyzed the possibility of using triticale pulp in packaging paper as a printing substrate based on the stability of black offset print under the influence of artificial aging, rubbing, and chemical treatment.

## 2. Materials and Methods

### 2.1. Raw Materials and Laboratory Production of Paper Substrates

According to standard EN ISO 5269-2:2004 [13], circular paper sheets with a similar basis weight (42.5 g/m<sup>2</sup>) and diameter (200 mm) were formed by a Rapid-Köthen sheet former (FRANK-PTI). To produce the pulp needed for paper production, after the food grain harvest of a hybrid of rye and wheat (*Triticale* sp.) was complete, the straw left over was collected in the fields of central Croatia and manually cut into pieces of up to 3 cm long. This straw contained 92.3% dry matter, of which 5.27% was ash with an insignificant share of silicon derivatives (7.74 mg/kg) and 52.88% was Kuschner–Hoffer cellulose [11]. Purified from grain and impurities through the soda pulping process, triticale straw was converted into semi-chemical pulp [14]. Pulp made from recycled wood fibers, which is often used to make newsprint, served as the basis to produce laboratory paper. With the aim of improving its properties, primarily strength, the obtained unbleached triticale straw pulp was added in a percentage of 10%, 20%, and 30% so that the paper could be used for packaging. Four different types of laboratory-made papers were produced (Table 1), with 50 pieces for each type of paper.

**Table 1.** Classification and properties of paper substrates used in this research.

Mark	Pulp (%)		Roughness, $R_a$ ( $\mu\text{m}$ ) (ISO 4287:1997) [15]	Thickness ( $\mu\text{m}$ ) (ISO 534:2011) [14,16]	Brightness (ISO 2470-2) [17,18]	Yellowness Index, YI (ASTM E 313) [17,19]
	Recycled Wood Fibers	Triticale Fibers				
N	100	0	$2.66 \pm 0.34$	$94.0 \pm 2.79$	$58.12 \pm 0.02$	46.80
1NTR	90	10	$3.57 \pm 0.35$	$96.3 \pm 6.35$	$53.91 \pm 0.02$	51.28
2NTR	80	$3.74 \pm 0.39$	$98.3 \pm 6.68$	$50.58 \pm 0.11$	53.62	
3NTR	70	30	$3.81 \pm 0.49$	$99.4 \pm 6.20$	$48.49 \pm 0.06$	57.19

## 2.2. Printing

Ten paper samples of each type of laboratory-made paper were cut to dimensions of  $4 \times 20$  cm prior printing. All cut laboratory-made paper substrates (Figure 1a–d) were printed using the dry offset process, at a speed of 0.5 m/s and a pressure of 600 N, in full-tone black ink on a Prüfbau multipurpose printability testing machine with a quantity of  $1.1 \text{ cm}^3$  of low-migration ink Sun Pak FSP (manufacturer Sun Chemicals) on the distribution rollers with a viscosity of  $87.47 \pm 2.74 \text{ Pa}\cdot\text{s}$  at a temperature of  $23 \text{ }^\circ\text{C}$  and relative humidity of 50%, as shown in Figure 1e–h. The printing for the purpose of this research was carried out in accordance with the ISO 12647-2:2013 standard, i.e., FOGRA PSO (ISO/TC 130 Graphic technology, 2013) [20]. All obtained prints reached the recommended standard values CIE  $L^*a^*b^*$  with a tolerance level of  $\Delta E^*_{ab} = 2$ . Before print stability assessment, all printed laboratory-made paper substrates were dried through oxidation polymerization for 24 h in the same ambient conditions used for printing.

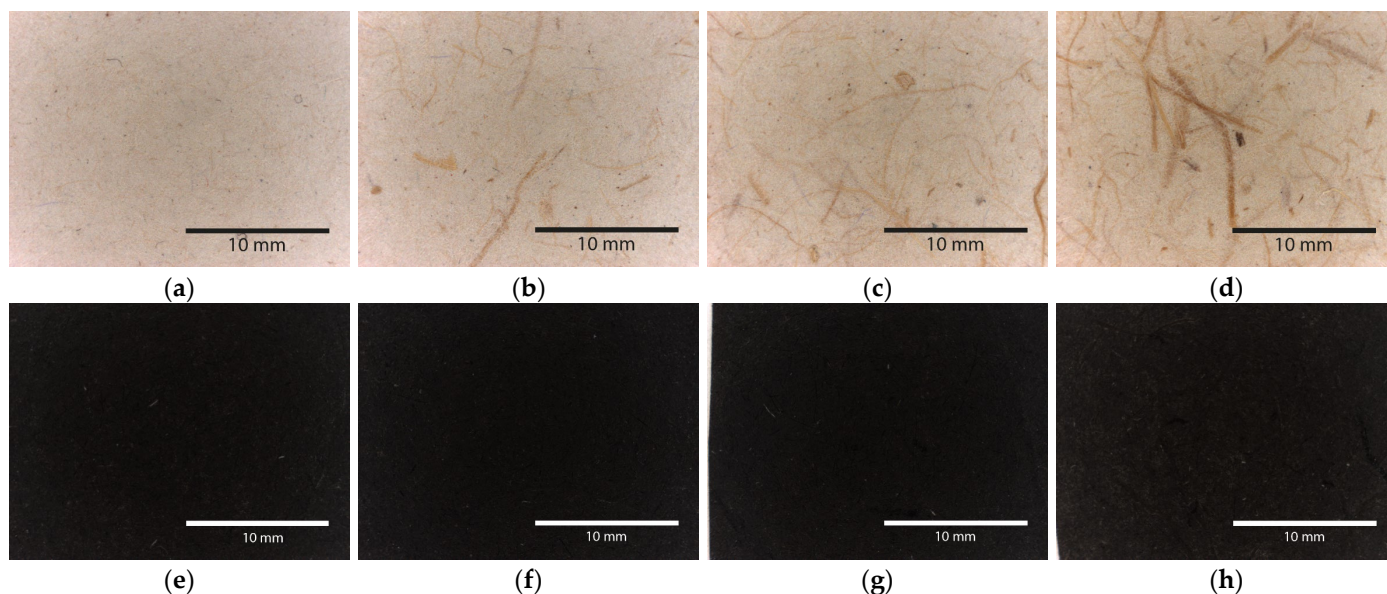


**Figure 1.** Microscopic images of laboratory-made papers substrates: (a) N; (b) 1NTR; (c) 2NTR; (d) 3NTR and black offset prints on (e) N; (f) 1NTR; (g) 2NTR; (h) 3NTR paper substrates.

## 2.3. Print Stability Assessment

High-quality reproductions and the stability of prints depend on the requirements of the manufacturer of packaged goods. To achieve them, it is necessary to be aware of the characteristics of the paper substrate and the possibilities of a particular printing technique. In this context, three stability assessment treatments (aging, rubbing, and treatment with chemical agents) were performed on papers with triticale pulp printed using the offset technique. The evaluation of aging, rubbing, and chemical resistance of offset prints on papers with triticale straw pulp was based on the color difference ( $\Delta E^*_{ab}$ ), which was calculated according to Equation (1). Specific ink color components CIE  $L^*$ ,  $a^*$ , and  $b^*$  were

measured using the spectrophotometer X-Rite SpectroEye before and after each treatment under illuminant D50, 2° standard observer.

$$\Delta E_{ab}^* = \sqrt{(L_2^* - L_1^*)^2 + (a_2^* - a_1^*)^2 + (b_2^* - b_1^*)^2} \quad (1)$$

where  $\Delta E_{ab}^*$  is the total color difference,  $L_1^*$ ,  $a_1^*$ , and  $b_1^*$  represent color values before each treatment, and  $L_2^*$ ,  $a_2^*$ , and  $b_2^*$  represent the color values measured after each treatment.

The results of change in visual perception of color due to the aging, rubbing, or chemical treatments are given as an average of ten measurements on each print sample. The interpretation of  $\Delta E_{ab}^*$  from the point of view of print quality in the graphics industry is listed in Table 2 [21].

**Table 2.** Interpretation of  $\Delta E_{ab}^*$  value.

$\Delta E_{ab}^*$ Value	Color Perception	Tolerance
≤1.0	Differences in color are unrecognizable by a standard observer.	Acceptable for graphics industry.
1–2	Only an experienced observer can perceive the differences.	
2–3.5	An inexperienced observer can perceive the differences.	Not acceptable for graphics industry.
3.5–5	Every observer can easily see the difference.	
>5	An observer recognizes two different colors.	

If the value of the color differences ( $\Delta E_{ab}^*$ ) of prints after aging, rubbing, or chemical treatment is less than 2, it is defined as a stable print with very small or small noticeable differences in the tone that can be recognized by a standard observer. When the value of the color difference increases (greater than 2), the change in color is more clearly visible for a standard observer, and the sample can be defined as a print with low resistance to aging, rubbing, or chemical agents.

### 2.3.1. Aging Treatment

Offset prints were cut into strips of 20 mm × 50 mm and placed side by side in a Suntest XLS+ test chamber, which was equipped with a daylight filter that emitted visible and near-ultraviolet electromagnetic radiation in a wavelength range from 290 nm to 800 nm. The artificial aging procedure was carried out according to ASTM D 6789-02 [22], where the level of light intensity was  $765 \pm 50$  W/m<sup>2</sup>, the temperature in the test chamber was up to 39.5 °C, and the relative humidity was 50%. Exposure to radiation was performed in two cycles for 48 h and information about the aging course is given in Table 3.

**Table 3.** Course of aging in the Suntest XLS+ test chamber.

Aging Cycle No.	Time of Aging (h)	Dose of Energy Supplied (kJ/m <sup>2</sup> )	Natural Aging Comparable Time (Days)
1	48	132,192	44.5
2	96	264,384	89.0

According to the aging conditions used in this research, every hour spent in the Suntest XLS+ test chamber corresponds to a dose of energy absorbed of 2754 kJ/m<sup>2</sup>, which is compatible with approximately 22 h of natural aging [23]. This is in correlation with the statement that one hour of treatment under a xenon lamp corresponds to one day in nature [24,25].

In addition to the colorimetric values CIE  $L^*$ ,  $a^*$ , and  $b^*$  measured to calculate the total color difference  $\Delta E_{ab}^*$  (Equation (1)), the difference in color lightness values after the 48 h

and 96 h aging treatment ( $\Delta L^*_{48-0}$  and  $\Delta L^*_{96-0}$ ) and difference in color attributes  $a^*$  and  $b^*$  ( $\Delta a^*_{48-0}$ ,  $\Delta a^*_{96-0}$ ,  $\Delta b^*_{48-0}$  and  $\Delta b^*_{96-0}$ ) were calculated according to Equations (2)–(4):

$$\Delta L^*_{48-0} = L^*_{48} - L^*_0 \quad \Delta L^*_{96-0} = L^*_{96} - L^*_0 \quad (2)$$

$$\Delta a^*_{48-0} = a^*_{48} - a^*_0 \quad \Delta a^*_{96-0} = a^*_{96} - a^*_0 \quad (3)$$

$$\Delta b^*_{48-0} = b^*_{48} - b^*_0 \quad \Delta b^*_{96-0} = b^*_{96} - b^*_0 \quad (4)$$

Measurements of the amount of light reflected from the surface of the black ink layer on all papers before and after artificial aging were made using the same spectrophotometer, an X-Rite SpectroEye. The result is a dataset of reflectance values representing the spectral distribution of the light reflected from the point of the measurement. This procedure was then repeated for the entire spectrum and the resulting dataset can be visualized as a spectral curve, ranging from 400 nm to 700 nm and sampled every 10 nm. A difference in reflectance ( $\Delta R$ ) was observed after samples were artificially aged for 48 h ( $R_{48}$ ) and 96 h ( $R_{96}$ ) compared to prints that were not aged ( $R_0$ ). The reflectance difference was determined according to Equation (5):

$$\Delta R_{48-0} = R_{48} - R_0 \quad \Delta R_{96-0} = R_{96} - R_0 \quad (5)$$

Fourier transform infrared spectroscopy (FTIR) absorbance spectra were recorded within the 4000–400  $\text{cm}^{-1}$  range at a 4  $\text{cm}^{-1}$  resolution and averaged over 15 scans for the laboratory-made printing substrates and offset prints before and after the artificial aging test. The experiment was performed with the use of a Shimadzu FTIR IRAffinity-21 spectrometer.

### 2.3.2. Rub Treatment

After printing, all prints were completely dried before performing rub treatment. All prints were cut into smaller round samples with a diameter of 5 cm and subjected to a mechanical resistance test (i.e., rub treatment) on a Hanatek T4 Rub and Abrasion Tester in accordance with the standard BS 3110 [26] under a constant pressure of 0.23 kg (0.5 lb) with 20, 40, and 60 circular motions at a constant speed of one rotation per second. The lowest pressure available on the device was used as a simulation of handling this packaging. This test is based on the effect of the repeated relative movement of two contact surfaces under applied pressure (rubbing) and observation damage to a relatively thin layer of ink at the contact position and contamination of the unprinted parts of the opposite paper. After testing, all prints were analyzed with a spectrophotometer for their  $L^*$ ,  $a^*$ , and  $b^*$  values and by calculating the color difference,  $\Delta E^*_{ab}$ , while the opposite unprinted paper and its black ink traces were used to visually confirm the gradual ink transfer that corresponds to the number of rotations in the rub treatment.

### 2.3.3. Chemical Treatment

All printed laboratory papers were tested for their resistance to different inorganic and organic chemical agents in accordance with the international standard ISO 2836:2004 in the field of printing industry [27], with the exact procedure prescribed for each type of chemical agent. Of all listed chemical agents in the international standard ISO 2836:2004, six were chosen for chemical treatment as they are more likely to come into contact with the packaging paper during handling, transport, or storage. First, all printed samples were cut to a dimension of 2 cm  $\times$  5 cm, and the chemical stability treatments were carried out as follows. The sample was placed on the lower glass plate between two or four strips of filter paper previously soaked in liquid chemical agent (where the number of filter paper strips was defined by the type of liquid chemical agent used—for sodium hydroxide and acetic and citric acid, the total number of filter paper strips was two, while for water and soybean oil, it was four). Finally, the upper glass plate was placed on top and weighted

with a 1 kg weight. The contact time for each chemical agent is defined and, together with the data on liquid chemical agent concentration, summarized in Table 4.

**Table 4.** Course of aging in the Suntest XLS+ test chamber.

Chemical Agent	Concentration % by Volume	Receptor Surface	Contact Conditions	Treatment Time (min)
Water (H <sub>2</sub> O)	100			1440
Soybean oil	100			1440
Citric acid (C <sub>6</sub> H <sub>8</sub> O <sub>7</sub> )	5	filter paper	1 kg on 54 cm <sup>2</sup>	60
Acetic acid (CH <sub>3</sub> COOH)	5			30
Sodium hydroxide (NaOH)	1			10
Ethanol (C <sub>2</sub> H <sub>5</sub> OH)	96	glass tube	-	5

At the end of the contact time, each printed sample treated with sodium hydroxide or acetic or citric acid was washed with distilled water and dried in an oven at 50 °C for 30 min. The samples treated with water or soybean oil were immediately dried in an oven at 40 °C for 30 min. As can be seen from Table 4, for the ethanol stability assessment, the procedure was completely different, as the prints were not placed between soaked filter paper strips but were immersed in a glass tube containing ethanol for 5 min. Samples treated with alcohol were also dried in an oven at 40 °C for 5 min.

After chemical contact with inorganic and organic chemical agents, all prints were analyzed with a spectrophotometer for their  $L^*$ ,  $a^*$ , and  $b^*$  values and by calculating the color difference  $\Delta E^*_{ab}$ .

### 3. Results

Colorimetric values of the offset prints that were used for print stability assessment after aging, rubbing, and chemical treatment are presented in Table 5 as the average result of 50 measurements. In the CIE  $L^*a^*b^*$  color system, the differences in colors and their position are given by the color coordinates  $L^*$ ,  $a^*$ , and  $b^*$ . Here, the  $L^*$  axis indicates lightness from black to white ( $L^* = 0$  for black,  $L^* = 100$  for white), the  $a^*$  axis represent chromaticity from red to green (positive values are red, negative values are green) axis, and the  $b^*$  axis represent chromaticity from yellow to blue (positive values are yellow, negative values are blue). The  $a^*$  and  $b^*$  axes have no specific numerical limits.

**Table 5.** Colorimetric values of the paper samples printed with black ink.

Mark	$L^*$	$a^*$	$b^*$
N	30.01 ± 0.61	1.31 ± 0.02	3.47 ± 0.12
1NTR	28.72 ± 0.38	1.28 ± 0.03	3.15 ± 0.10
2NTR	29.04 ± 0.46	1.32 ± 0.05	3.48 ± 0.23
3NTR	34.63 ± 1.15	1.51 ± 0.03	5.49 ± 0.46

In order to determine whether there is an effective and, thus, visible color change under the influence of light and radiation, the color lightness values ( $L^*$ ) and, furthermore, the total color change ( $\Delta E^*_{ab}$ ) of all black prints were tested independently. The variance in lightness values ( $\Delta L^*$ ) and the total color changes ( $\Delta E^*_{ab}$ ) of the prints on all analyzed paper substrates obtained after artificial aging treatments of 48 and 96 h, in comparison with the values presented in Table 5, are shown in Figure 2.

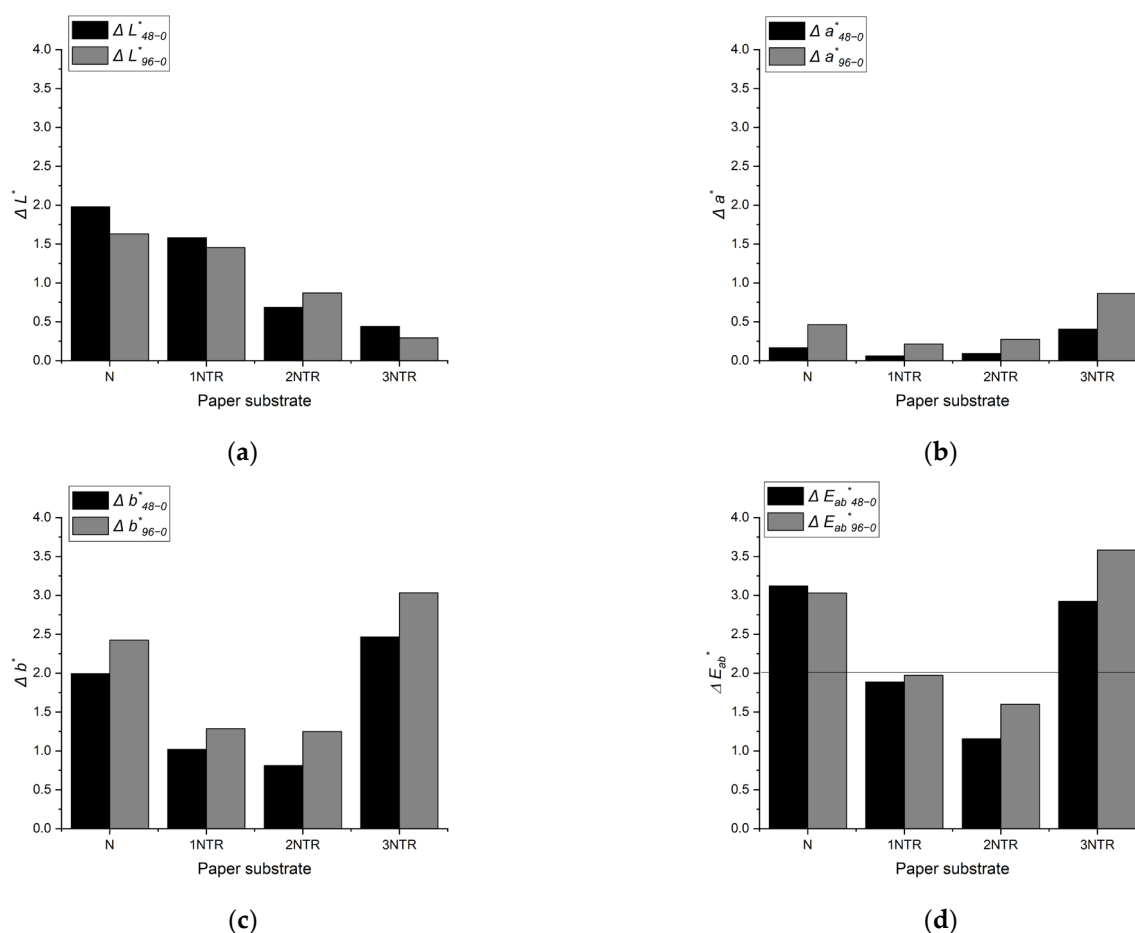


**Figure 2.** Influence of aging treatments of 48 h and 96 h on prints: (a) lightness difference ( $\Delta L^*$ ); (b) difference in color attribute  $a^*$  ( $\Delta a^*$ ); (c) difference in color attribute  $b^*$  ( $\Delta b^*$ ); (d) the total color difference ( $\Delta E^*_{ab}$ ).

The reflectance spectrum of each analyzed paper substrate, without (N) and with the addition of triticale straw pulp (1NTR, 2NTR, and 3NTR), and the reflectance spectrum of the printed paper substrates ( $N_0$ ,  $1NTR_0$ ,  $2NTR_0$ , and  $3NTR_0$ ) are shown in Figure 3a,b.

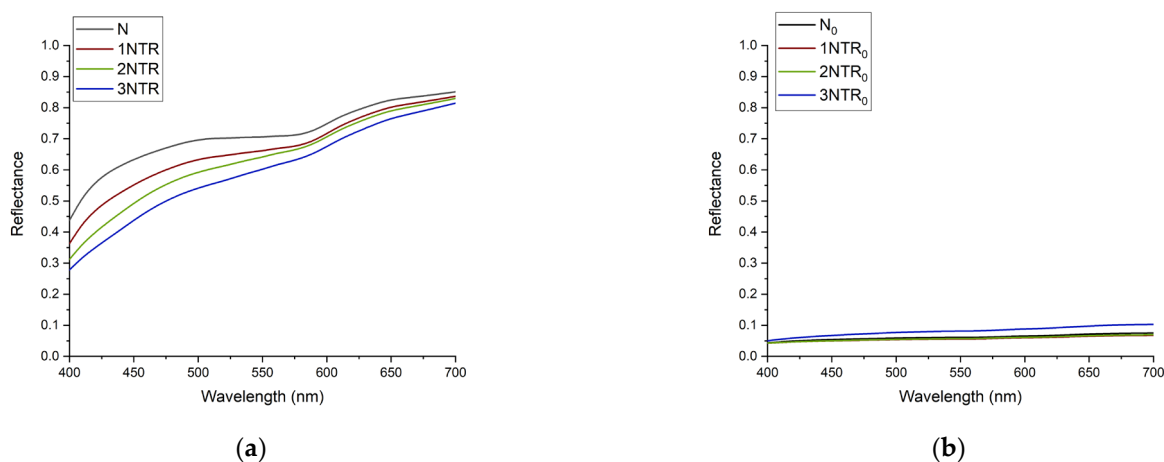


**Figure 3.** Reflectance spectrum of: (a) unprinted paper substrates; (b) prints on all paper substrates.

The variance in the visible reflectance spectra of ink film upon artificial aging for 48 h and 96 h is presented in Figure 4.

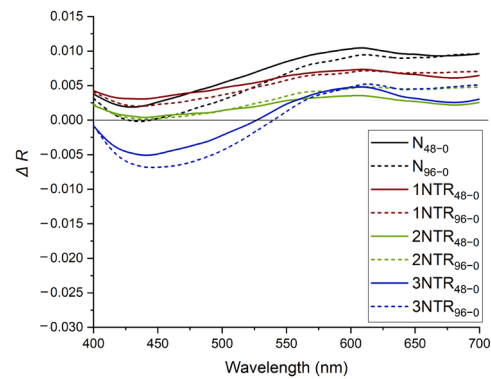
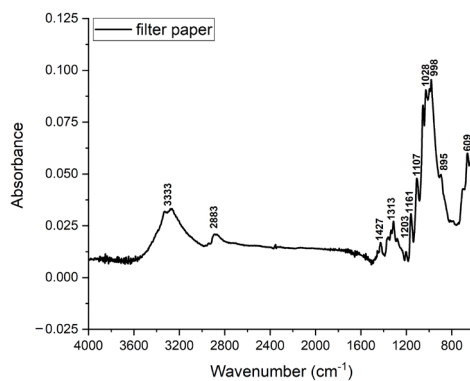
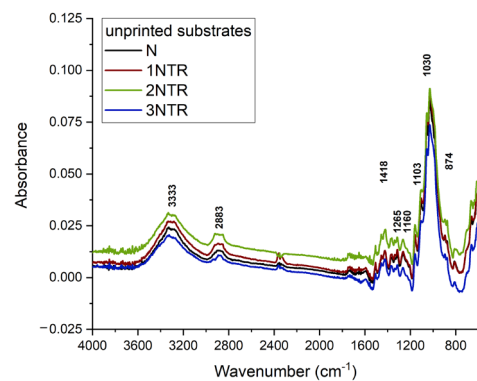


**Figure 4.** Reflectance difference ( $\Delta R$ ) after artificial aging of prints made on all analyzed paper substrates for 48 h and 96 h.

The FTIR spectrum of filter paper, as a reference for regions with the signals of cellulose macromolecules, is presented in Figure 5a, while FTIR spectra of the analyzed unprinted paper substrates are presented in Figure 5b.



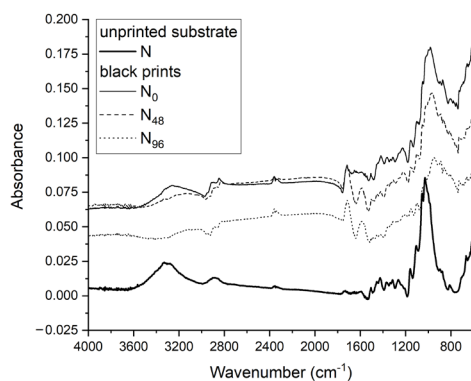
(a)



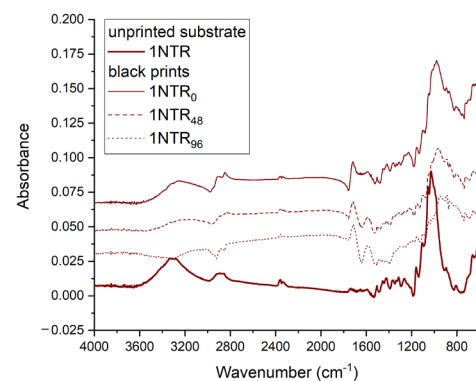
(b)

**Figure 5.** FTIR spectra of (a) filter paper; (b) unprinted papers substrates.

Changes that occurred during artificial ageing in two cycles of 48 h on prints on each analyzed paper substrate were observed through the FTIR spectra of the prints, and absorbance spectra are presented in Figure 6a–d.



(a)



(b)

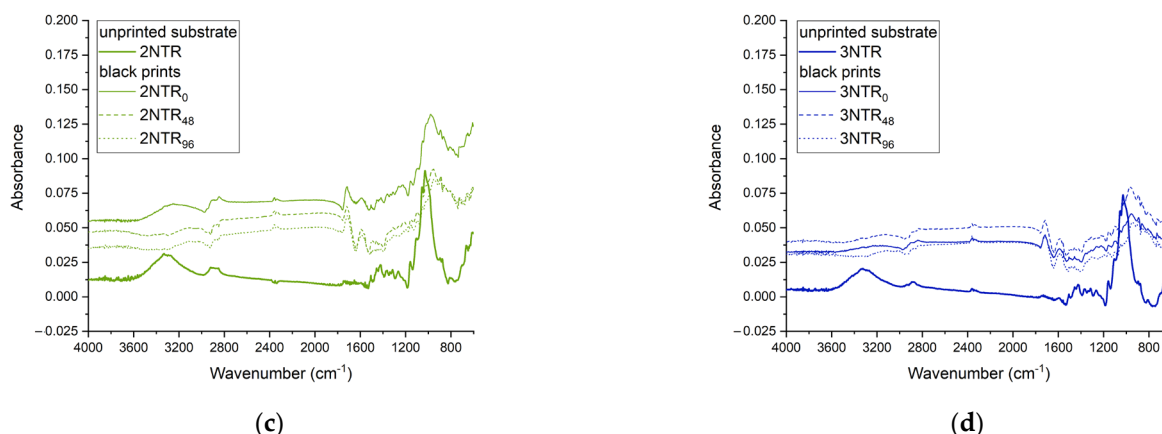


**Figure 6.** FTIR spectra of prints before and after artificial aging regarding paper substrate: (a) reference (N); (b) 1NTR; (c) 2NTR; (d) 3NTR. Note: In the legend, the 0 refers to unaged prints, the 48 refers to prints artificially aged for 48 h, and the 96 to prints artificially aged for 96 h.

The variance in total color differences,  $\Delta E_{ab}^*$ , of ink film upon rubbing treatment performed at different rotation numbers (20, 40 and 60) is presented in Figure 7. Given that one of the most common parameters that affects print rubbing is the roughness of the paper substrate surface, this element is also included in the presentation of results.

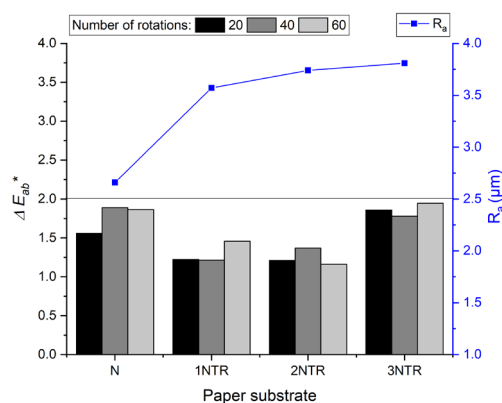
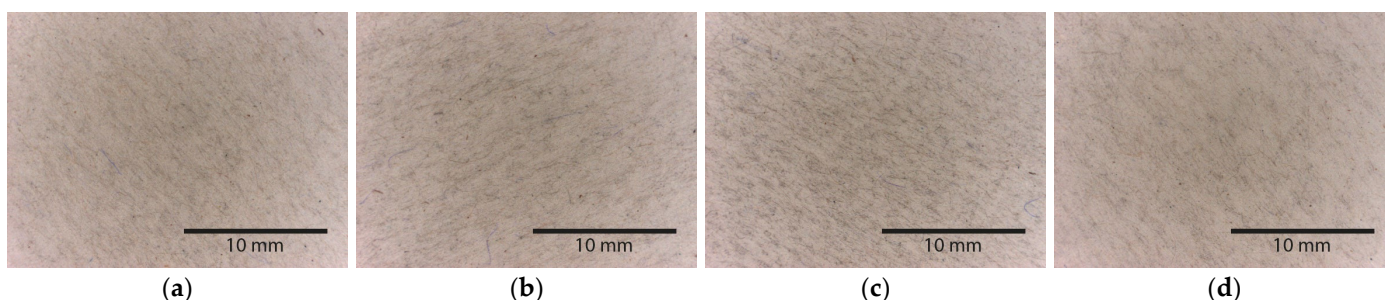


**Figure 7.** Color difference ( $\Delta E_{ab}^*$ ) of the prints after rub resistance testing with 20, 40, and 60 rotations in comparison with roughness of the unprinted paper ( $R_a$ ).

For a visual confirmation of the black ink transfer from all printed paper substrates (N, 1NTR, 2NTR, 3NTR) to the opposite contact surface as a result of rubbing, Figure 8a–l shows microscopic images of the paper contact surfaces after rubbing the prints at 20, 40, and 60 rotations.



(a)

(b)

(c)

(d)

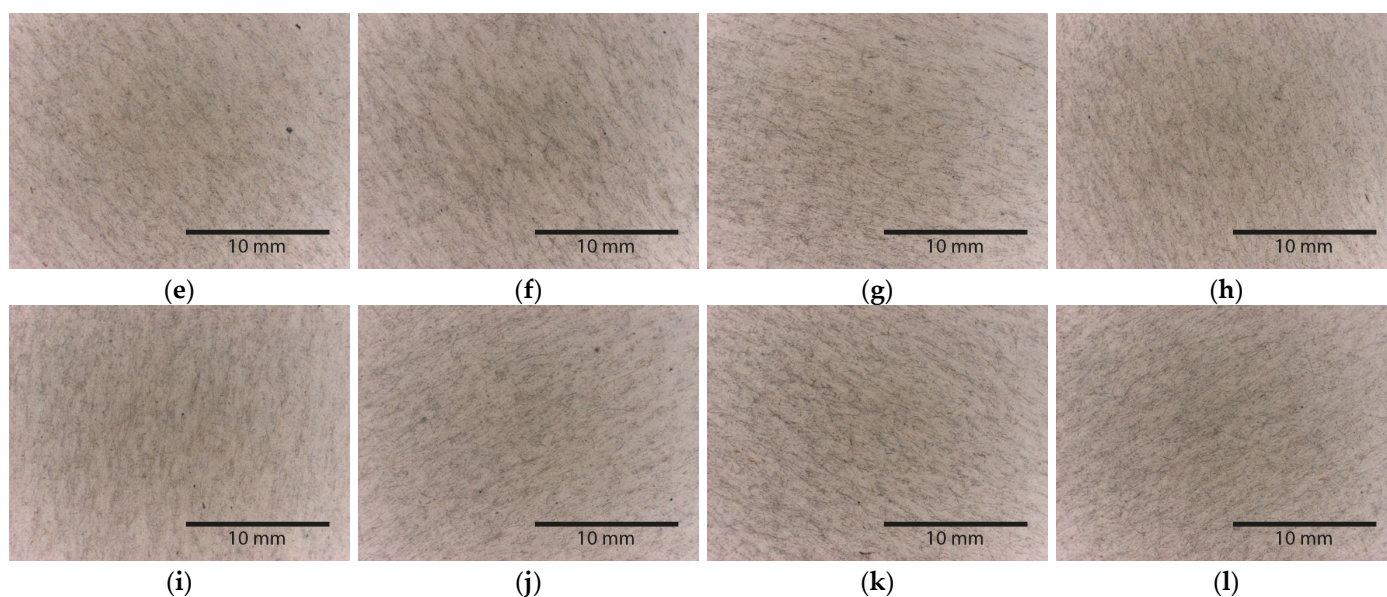


**Figure 8.** Microscopic images of the opposite paper surface after performing rubbing test on printed paper substrate: (a) N with 20 rotations; (b) 1NTR with 20 rotations; (c) 2NTR with 20 rotations; (d) 3NTR with 20 rotations; (e) N with 40 rotations; (f) 1NTR with 40 rotations; (g) 2NTR with 40 rotations; (h) 3NTR with 40 rotations; (i) N with 60 rotations; (j) 1NTR with 60 rotations; (k) 2NTR with 60 rotations; (l) 3NTR with 60 rotations.

The variance in total color differences ( $\Delta E^*_{ab}$ ) of black ink film upon treatment with inorganic and organic chemical agents is presented in Figure 9a,b.

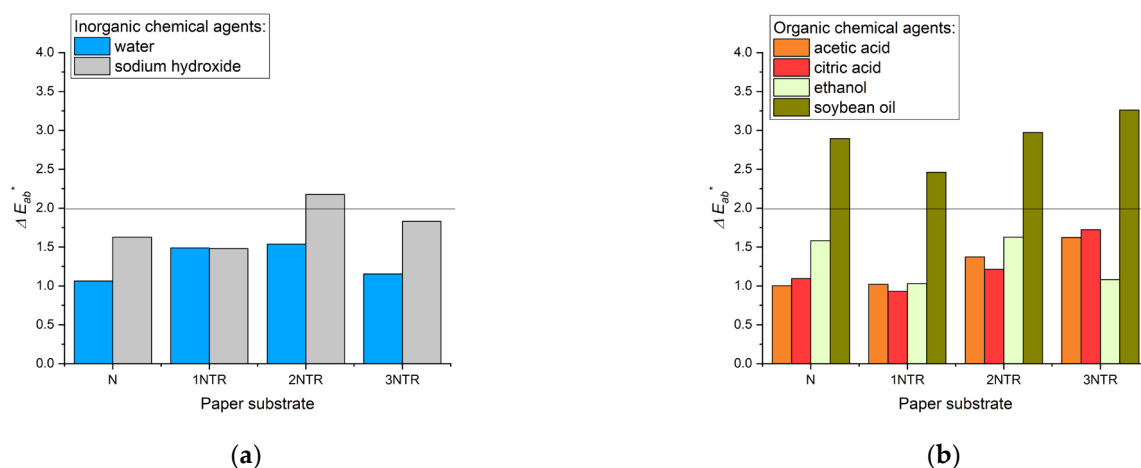


**Figure 9.** Color difference ( $\Delta E^*_{ab}$ ) of the prints after treatment with (a) inorganic chemical agents; (b) organic chemical agents.

#### 4. Discussion

Given that print stability is of utmost importance for packaging materials, an overall stability assessment of printed packaging paper containing triticale straw pulp was conducted based on aging, rubbing, and chemical stability.

The impact of artificial aging through two cycles of 48 h each was observed through the changes in the colorimetric values of the black color print:  $\Delta L^*$  (Figure 2a),  $\Delta a^*$  (Figure 2b), and  $\Delta b^*$  (Figure 2c), and that regarding numerically easily visible tolerance for the graphics industry through the total color change ( $\Delta E^*_{ab}$ ) (Figure 2d). Although the biggest changes in the CIE  $L^*a^*b^*$  color space were expected for the lightness color value, given that the research was carried out on black prints, this was not the case. Moreover, it was observed that the black print on laboratory-made sustainable paper has a more stable

lightness as the proportion of triticale straw pulp increases. It was also observed that the most significant changes related to this color parameter occur within the first 48 h, while further aging has an insignificant effect on the lightness value, regardless of the type of printing substrate used (Figure 2a). It can be seen from Figure 2b that the color attribute  $a^*$  of black prints does not change significantly after the first cycle of artificial aging on any printing substrate, while an additional 48 h of aging leads to a somewhat greater change, especially when printed on a paper substrate with 30% triticale pulp. It is obvious that the paper substrate plays a significant role in the stability of the black color after the aging of offset prints. Since the pulp was not subjected to a bleaching process and was obtained through semi-chemical pulping of the cereal straw, the residual lignin remained in the pulp, which caused yellowing and reddening of the formed paper during aging. Therefore, the aged prints show a shift in color measurement in the positive direction along the  $a^*$  and  $b^*$  axes in the CIE color space, indicating a shift toward red and yellow hues. The most significant is the shift along the  $b^*$  axis, which indicates the yellowing of prints due to aging. An identical trend to that of the changes caused by artificial aging observed for the  $b^*$  color attribute (Figure 2c) was also observed for the total color difference (Figure 2d) calculated according to Equation (1), confirming that for prints on laboratory-made sustainable paper containing triticale straw pulp, it is exactly the  $b^*$  color attribute that is most responsible for the change in  $\Delta E^*_{ab}$ . The appearance of yellowing of the black print due to artificial aging can certainly be correlated with the composition of the paper substrate, for which an increase in the yellowness index (Table 1) of up to 22.2% was determined for the laboratory-made paper substrate with the maximum addition of unbleached triticale straw pulp of 30% compared with the paper substrate without the addition of triticale straw pulp (N). However, the overall color difference  $\Delta E^*_{ab}$  of all prints showed good stability ( $\Delta E^*_{ab} \leq 3.58$ ) under the given artificial aging conditions. Figure 2d shows how prolonging the aging treatment of prints on all paper substrates leads to further degradation of the print.

Figure 3 shows the reflectance spectra of the analyzed laboratory-made paper substrates (Figure 3a) and the prints made on them (Figure 3b). Since the optical properties of paper are very sensitive to its structure, the absorption of the paper substrate depends largely on the content of cellulose, hemicellulose, and lignin. In general, lignin absorbs more strongly than cellulose or hemicellulose in the UV and visible spectral range due to its aromatic nature [28]. Pure cellulose and hemicellulose absorb more significantly in the near UV spectral range (300–380 nm) than in the visible spectral range (380–550 nm) [29,30]. It was noticed that in the range of shorter wavelengths, all analyzed paper substrates show a lower reflectance, and their reflectance values decrease with a higher proportion of triticale straw pulp. On the other hand, the black prints on analyzed paper substrates have negligible reflections in the entire visible part of the spectrum, i.e., it can be concluded that the black ink absorbs light energy uniformly over the entire range of the visible spectrum. This is also confirmation that the black ink was printed on all substrates with high quality. After both aging cycles (48 h and 96 h), the reflectance spectra of prints on all paper substrates are characterized by an increased reflectance (Figure 4). This behavior is in correlation with results obtained for offset black ink printed on alkaline offset paper aged with standard moist heat and dry heat treatments [31]. However, the shape of the spectrum for all prints contains minor changes for wavelengths below 500 nm, while more significant changes occur for wavelengths above 500 nm. The reflectance of all analyzed printed paper substrates gradually increases, and only the 3NTR paper substrate achieves a reduced reflectance up to 550 nm with the first aging cycle and a further reduction with the second aging cycle (96 h). From the shape of the spectrum, the greatest increased reflectance is evident in the red part of the spectrum, which confirms the changes observed in the analysis of the CIE  $L^*a^*b^*$  colorimetric values.

The outcome of the FTIR analysis of filter paper is shown in Figure 5a and Table 6. FTIR spectra of filter paper made from pure cellulose fibers were obtained to better identify the regions where cellulose macromolecule signals are recorded.

**Table 6.** Values of wavenumbers attributed to the chemical moieties [32].

Wavenumber (cm <sup>-1</sup> )	Chemical Group
3333	$\gamma$ OH covalent bond, hydrogen bonding
2883	$\gamma$ CH
1427	$\delta$ CH <sub>2</sub> (symmetric) at C-6; crystalline region
1313	$\delta$ CH <sub>2</sub> (wagging) at C-6
1203	$\delta$ COH in plane at C-6
1161	$\gamma$ COC at $\beta$ -glycosidic linkage
1107	$\gamma$ ring in plane
1028	$\gamma$ CO at C-6
895	$\gamma$ COC at $\beta$ -glycosidic linkage; amorphous region
609	$\delta$ COH out of plane

Figure 5b shows an FTIR spectra of the unprinted paper substrates N, 1NTR, 2NTR, and 3NTR, respectively. Since all analyzed printing substrates contain calcium carbonate as a filler in higher or lower content, the band that appears at 874 cm<sup>-1</sup> is the calcium carbonate vibrational band [33–35].

From the FTIR spectra presented in Figure 6a–d, it is evident that the changes in the chemical moieties are caused by the application of the ink to the substrates through the offset printing process. The largest change in the FTIR spectrum after printing was observed for all paper substrates at a wavenumber ranging from 1750 cm<sup>-1</sup> to 1100 cm<sup>-1</sup>, which was caused by the applied ink. Offset black ink shows similar peaks of its FTIR spectra to the commercial gravure printing ink reported by Ramli et al. corresponding to chemical functional groups. For the C=O functional group, the peak was recorded at 1716 cm<sup>-1</sup>, for the C-H functional group, it was recorded at 1456 cm<sup>-1</sup> and 1355 cm<sup>-1</sup>, and for the C-O and C-O-C functional groups, the peaks were recorded at 1225 cm<sup>-1</sup> and 1097 cm<sup>-1</sup> [36]. On the other hand, the pronounced peaks at 3333 cm<sup>-1</sup> related to hydrogen bonds of native cellulose and at 2883 cm<sup>-1</sup> related to carbon–hydrogen bonds (most likely  $\gamma$ CH vibrations of methylene in cellulose) of paper as a printing substrate are broadened by printing, i.e., peak broadening occurs. Peak broadening is an indication of the degradation of the crystalline structure of the cellulose catalyzed by either the chemistry of the ink or the binding mechanism of the ink to the paper substrate. Along with artificial aging, the absorption curves for all analyzed paper substrates were changed, regardless of whether triticale straw pulp was added to them or not. The vibrational bands occurring at 3333 cm<sup>-1</sup> and 2883 cm<sup>-1</sup> gradually weaken with aging, as the initiated reaction of the degradation of the cellulose structure is further enhanced by the effect of aging, where the dehydration of the cellulose certainly occurs, while all samples revealed a rising peak at 1716 cm<sup>-1</sup>, becoming stronger due to the vibrations of the C=O functional group [35].

The results of the rub stability of printed sustainable paper substrates presented in Figure 7 showed that all printed paper substrates, regardless of whether they contained triticale pulp or not, achieved the greatest color changes after the initial 20 rotations, and after further series of rub cycles (40 and 60), the color changes reached a maximum of 28%. The penetration of the ink increases with increased surface roughness [37], and as the addition of virgin triticale straw fibers to a pulp of recycled fibers increases the surface roughness parameter R<sub>a</sub> of the paper substrate (from 2.66 for N to 3.81 for 3NTR), it was expected that as the roughness of the printing substrate increases, the stability of the print on rubbing will decrease. In general, for all prints, changes in the color increase with the number of rubbing cycles. It is interesting to note that printed paper substrates with 10% and 20% triticale pulp show about the same rub resistance of the print after 20 rotations ( $\Delta E^*_{ab} \approx 1.22$ ), which is only perceptible for an experienced observer. It is certainly important to emphasize that regardless of whether the prints were made on paper substrates without or with triticale pulp, at 60 rotations in total, all analyzed prints showed sufficient rub resistance, with  $\Delta E^*_{ab}$  below the threshold value of 2. Images of the opposite contact

surface of the paper (Figure 8a–l) used for the black print rubbing test at different rotations on reference paper (N) and papers with triticale straw pulp (1NTR, 2NTR and 3NTR) intended for sustainable packaging confirm that the black print obtained is resistant to mechanical rubbing because there is no significant ink transfer, which is of high importance for printed packaging. From this and from our previous studies, it can be concluded that laboratory paper substrates with straw pulp addition up to 30% has satisfactory stability of prints in rub resistance tests and can be recommended for further development in the production of paper for packaging and other purposes.

When considering the chemical resistance of the prints, which is important for the packaging of liquid products, the black offset prints were very stable in contact with all the inorganic chemical agents used (Figure 9a), while in the case of the organic chemical agents (Figure 9b), the printed paper substrates changed color in contact with soybean oil, whereby the obtained color difference value ( $\Delta E^*_{ab}$ ) was greater than 2, which can be perceived by an inexperienced observer. The highest color change value ( $\Delta E^*_{ab} = 3.26$ ) was observed on printed paper substrates with 30% triticale pulp (3NTR). Overall, printed paper substrates with the addition of triticale straw pulp (1NTR, 2NTR, 3NTR) achieved the same chemical stability as printed paper substrates made only from recycled fibers (N).

## 5. Conclusions

In terms of greater environmental consciousness, the addition of virgin straw fibers to the pulp of recycled fiber provides a distinct advantage by reducing the use of virgin wood fibers, and also by reducing waste from agricultural processes. Based on the research conducted on printed paper substrates with the addition of triticale pulp, we can draw several conclusions:

- After the artificial aging procedure, it was found that the black print on the paper substrates has more stable lightness regardless of the increase in the proportion of triticale straw pulp, while greater changes in hue were observed, giving the print a more yellowish and reddish appearance after aging. This behavior was also confirmed when the differences in reflectance were shown by subtracting the reflectance spectrum after aging and the reflectance spectrum before aging. FTIR analysis revealed that the absorption curve changes equally with aging for all analyzed paper substrates, regardless of whether triticale pulp was added to them or not. The vibration bands occurring at  $3333\text{ cm}^{-1}$  and  $2883\text{ cm}^{-1}$  disappear with increasing aging time.
- The mechanical stability of all printed paper substrates, regardless of whether they contain triticale straw pulp or not, reaches the greatest color changes after the initial 20 rotations, with the most stable prints produced on paper substrates containing 10% and 20% triticale straw pulp. All analyzed prints meet the rubbing resistance after a cycle of 60 rotations, which an inexperienced observer cannot notice as changes in the color of the prints.
- All the observed black offset prints achieve very good stability in contact with all the inorganic chemical agents used, while in the case of the organic chemical agents, the printed paper substrates changed color more significantly after contact with soybean oil, which is noticeable even by an inexperienced observer.
- Considering the results obtained, it can be concluded that printed paper substrates with the addition of triticale straw pulp can be used for sustainable packaging of products that do not contain soybean oil.

**Author Contributions:** Conceptualization, M.R., I.P. and I.B.; methodology, M.R., I.P. and I.B.; formal analysis, M.R., I.P., I.B. and K.P.M.; investigation, M.R., I.P., I.B. and K.P.M.; resources, M.R., I.P., I.B. and K.P.M.; writing—original draft preparation, M.R.; writing—review and editing, I.P. and I.B.; visualization, I.P. and M.R.; supervision, I.B.; project administration, I.B.; funding acquisition, I.B. All authors have read and agreed to the published version of the manuscript.

**Funding:** This research was funded by the Croatian Science Foundation, grant number UIP-2017-05-2573.

**Data Availability Statement:** Not applicable.

**Acknowledgments:** The authors would like to thank Valentina Radić Seleš for her technical support. This work has been supported, in part, by the Croatian Science Foundation under the project “Printability, Quality and Utilization of Substrates with Non-Wood Fibres” (UIP-2017-05-2573).

**Conflicts of Interest:** The authors declare no conflict of interest.

## References

1. Steenis, N.D.; van Herpen, E.; van der Lans, I.A.; Ligthart, T.N.; van Trijp, H.C.M. Consumer response to packaging design: The role of packaging materials and graphics in sustainability perceptions and product evaluations. *J. Clean. Prod.* **2017**, *162*, 286–298. <https://doi.org/10.1016/j.jclepro.2017.06.036>.
2. Ertz, M.; François, J.; Durif, F. How consumers react to environmental information: An experimental study. *J. Int. Consum. Mark.* **2017**, *29*, 162–178. <https://doi.org/10.1080/08961530.2016.1273813>.
3. Oloyede, O.O.; Lignou, S. Sustainable paper-based packaging: A consumer’s perspective. *Foods* **2021**, *10*, 1035. <https://doi.org/10.3390/foods10051035>.
4. CEPI Preliminary Statistics. 2022. Available online: [https://www.cepi.org/wp-content/uploads/2023/02/Cepi\\_Preliminary-statistics-2022\\_15022023.pdf](https://www.cepi.org/wp-content/uploads/2023/02/Cepi_Preliminary-statistics-2022_15022023.pdf) (accessed on 25 March 2023).
5. EUROSTAT Statistical Report: Generation of Waste by Waste Category, Hazardousness and NACE Rev. 2 Activity. Available online: [https://ec.europa.eu/eurostat/databrowser/view/ENV\\_WASGEN\\_\\_custom\\_5688189/default/table?lang=en](https://ec.europa.eu/eurostat/databrowser/view/ENV_WASGEN__custom_5688189/default/table?lang=en) (accessed on 25 March 2023).
6. EUROSTAT Statistical Report: Packaging Waste by Waste Management Operations. Available online: [https://ec.europa.eu/eurostat/databrowser/view/ENV\\_WASPAC\\_\\_custom\\_5688161/default/table?lang=en](https://ec.europa.eu/eurostat/databrowser/view/ENV_WASPAC__custom_5688161/default/table?lang=en) (accessed on 25 March 2023).
7. Grilj, S.; Muck, T.; Hladnik, A.; Gregor-Svetec, D. Recycled papers in everyday office use. *Nord. Pulp Pap. Res. J.* **2011**, *26*, 349–355. <https://doi.org/10.3183/NPPRJ-2011-26-03-p349-355>.
8. McKinney, R.W.J. (Ed.) *Technology of Paper Recycling*; Springer: Dordrecht, The Netherlands, 1995; p. 401.
9. Abd El-Sayed, E.S.; El-Sakhawy, M.; El-Sakhawy, M.A.-M. Non-wood fibers as raw material for pulp and paper industry. *Nord. Pulp Pap. Res. J.* **2020**, *35*, 215–230. <https://doi.org/10.1515/npprj-2019-0064>.
10. Thakur, T.C.; Rajan, P. Availability of wheat straw in combine harvested fields for baling. *Agric. Eng. Today* **2001**, *25*, 1–14.
11. Plazonić, I.; Barbarić-Mikočević, Ž.; Antonović, A. Chemical composition of straw as an alternative material to wood raw material in fibre isolation. *Drv. Ind.* **2016**, *67*, 119–125. <https://doi.org/10.5552/drind.2016.1446>.
12. Malik, S.; Rana, V.; Joshi, G.; Gupta, P.K.; Sharma, A. Valorization of wheat straw for the paper industry: Pre-extraction of reducing sugars and its effect on pulping and papermaking properties. *ACS Omega* **2020**, *5*, 30704–30715. <https://doi.org/10.1021/acsomega.0c04883>.
13. *ISO 5269-2:2004*; Pulps—Preparation of Laboratory Sheets for Physical Testing—Part 2: Rapid-Köthen Method. International Organization for Standardization: Geneva, Switzerland, 2004.
14. Plazonić, I.; Bates, I.; Barbarić-Mikočević, Ž. The effect of straw fibers in printing papers on dot reproduction attributes, as realized by UV inkjet technology. *BioResources* **2016**, *11*, 5033–5049. <https://doi.org/10.15376/biores.11.2.5033-5049>.
15. *ISO 4287:1997*; Geometrical Product Specifications (GPS)—Surface Texture: Profile Method—Terms, Definitions and Surface Texture Parameters. International Organization for Standardization: Geneva, Switzerland, 1997.
16. *ISO 534:2011*; Paper and Board—Determination of Thickness, Density and Specific Volume. International Organization for Standardization: Geneva, Switzerland, 2011.
17. Plazonić, I.; Bates, I.; Vukoje, M. Changes in straw-containing laboratory papers caused by accelerated ageing. *Heritage* **2022**, *5*, 1836–1851. <https://doi.org/10.3390/heritage5030095>.
18. *ISO 2470-2:2008*; Paper, Board and Pulps—Measurement of Diffuse blue Reflectance Factor—Part 2: Outdoor Daylight Conditions (D65 Brightness). International Organization for Standardization: Geneva, Switzerland, 2008.
19. *ASTM E313*; Standard Practice for Calculating Yellowness and Whiteness Indices from Instrumentally Measured Color Coordinates. ASTM International: West Conshohocken, PA, USA, 2020.
20. *ISO 12647-2:2013*; Graphic Technology—Process Control for the Production of Half-Tone Colour Separations, Proof and Production Prints—Part 2: Offset Lithographic Processes. International Organization for Standardization: Geneva, Switzerland, 2013.
21. Mokrzycki, W.S.; Tatol, M. Color difference delta E—A survey. *Mach. Graph. Vis.* **2011**, *20*, 383–411.
22. *ASTM D6789-02*; Paper—Standard Test Method for Accelerated Light Aging of Printing and Writing Paper by Xenon-Arc Exposure Apparatus. ASTM International: West Conshohocken, PA, USA, 2017.
23. Plazonić, I.; Džimbeg-Malčić, V.; Bates, I.; Žilić, G. The effect of electromagnetic radiation on the reflectance spectra of prints on hemp papers. *J. Graph. Eng. Des.* **2021**, *12*, 21–28. <https://doi.org/10.24867/JGED-2021-2-021>.
24. Debeljak, M.; Gregor-Svetec, D. Optical and color stability of aged specialty papers and ultraviolet cured ink jet prints. *J. Imaging Sci. Technol.* **2010**, *54*, 060402-1–060402-9. <https://doi.org/10.2352/J.ImagingSci.Technol.2010.54.6.060402>.

25. Izdebska, J.; Żółek-Tryznowska, U.; Książek, T. Influence of artificial aging on cellulose film. The optical properties of printed and non-printed biodegradable film bases. *Agro Food Ind. Hi Tech* **2013**, *24*, 52–56.
26. BS 3110:1959; Graphic Technology—Inks. Printing Inks—Methods for Measuring the Rub Resistance of Print. BS Standards: Southampton, UK, 1959.
27. ISO 2836:2004; Graphic Technology—Prints and Printing Inks—Assessment of Resistance of Prints to Various Agents. International Organization for Standardization: Geneva, Switzerland, 2004.
28. Zervos, S.; Deprez, T.; Lejeune, A. (Eds.) *Cellulose: Structure and Properties, Derivatives and Industrial Uses*; Nova Publishing: New York, NY, USA, 2010; pp. 155–203.
29. Strlič, M.; Kolar, J. (Eds.) *Ageing and Stabilisation of Paper*; National and University Library: Ljubljana, Slovenia, 2005.
30. Malešič, J.; Kolar, J.; Strlič, M.; Kočar, D.; Fromageot, D.; Lemaire, J.; Haillant, O. Photo-induced degradation of cellulose. *Polym. Degrad. Stab.* **2005**, *89*, 64–69.
31. Havlínová, B.; Babiaková, D.; Brezová, V.; Ďurovič, M.; Novotná, M.; Belányi, F. The stability of offset inks on paper upon ageing. *Dye. Pigment.* **2002**, *54*, 173–188. [https://doi.org/10.1016/S0143-7208\(02\)00045-1](https://doi.org/10.1016/S0143-7208(02)00045-1).
32. Cichosz, S.; Masek, A. IR study on cellulose with the varied moisture contents: Insight into the supramolecular structure. *Materials* **2020**, *13*, 4573. <https://doi.org/10.3390/ma13204573>.
33. Bosch Reig, F.; Gimeno Adelantado, J.V.; Moya Moreno, M.C.M. FTIR quantitative analysis of calcium carbonate (calcite) and silica (quartz) mixtures using the constant ratio method. Application to geological samples. *Talanta* **2002**, *58*, 811–821. [https://doi.org/10.1016/S0039-9140\(02\)00372-7](https://doi.org/10.1016/S0039-9140(02)00372-7).
34. Rožič, M.; Šegota, N.; Vukoje, M.; Kulčar, R.; Šegota, S. Description of thermochromic offset prints morphologies depending on printing substrate. *Appl. Sci.* **2020**, *10*, 8095. <https://doi.org/10.3390/app10228095>.
35. Zghari, B.; Hajji, L.; Boukir, A. Effect of Moist and Dry Heat Weathering Conditions on Cellulose Degradation of Historical Manuscripts exposed to Accelerated Ageing: <sup>13</sup>C NMR and FTIR Spectroscopy as a non-Invasive Monitoring Approach. *J. Mater. Environ. Sci.* **2018**, *9*, 641–654. <https://doi.org/10.26872/jmes.2018.9.2.71>.
36. Ramli, S.; Talib, R.A.; Rahman, R.A.; Zainuddin, N.; Othman, S.H.; Rashid, N.M. Detection of lard in ink extracted from printed food packaging using Fourier transform infrared spectroscopy and multivariate analysis. *J. Spectrosc.* **2015**, *2015*, 502340. <https://doi.org/10.1155/2015/502340>.
37. Eriksen, Ø.; Johannesen, E.; Gregersen, Ø.W. The influence of paper surface roughness on ink pigment distribution. *Appita J.* **2007**, *60*, 384–389.

**Disclaimer/Publisher’s Note:** The statements, opinions and data contained in all publications are solely those of the individual author(s) and contributor(s) and not of MDPI and/or the editor(s). MDPI and/or the editor(s) disclaim responsibility for any injury to people or property resulting from any ideas, methods, instructions or products referred to in the content.